JCTC Journal of Chemical Theory and Computation

Article

pubs.acs.org/JCTC

How Evenly Can Approximate Density Functionals Treat the Different Multiplicities and Ionization States of 4d Transition Metal Atoms?

Sijie Luo and Donald G. Truhlar*

Department of Chemistry and Supercomputing Institute, University of Minnesota, Minneapolis, Minnesota 55455-0431, United States

ABSTRACT: The ability of density functional theory to predict the relative energies of different spin states, especially for systems containing transition metal atoms, is of great importance for many applications. Here, in order to sort out the key factors determining accuracy, we compare the predictions of 60 density functional approximations of 10 different types [local spin density approximation, generalized gradient approximation (GGA), nonseparable gradient approximation (NGA), global-hybrid GGA, range-separated hybrid GGA, range-separated hybrid GGA plus molecular mechanics, meta-GGA, meta-NGA, global-hybrid meta-GGA, and range-separated hybrid meta-GGA] for their ability to represent the spin-flip transitions of all 4d transition metal atoms of groups 3−10 (Y through Pd) and their singly positive cations. We consider all 16 excitation energies connecting the ground states (of the neutral atoms and the cations) to their first excited states of different multiplicities, and we also consider all eight ionization potentials. We also test the Hartree−Fock method. All density functional and Hartree−Fock calculations are converged to a stable solution, in which the spatial symmetry is allowed to be completely broken to achieve the lowest possible energy solution. By analyzing the fractional subshell occupancies and spin contaminations, we are able to sort out the effects of s orbital vs d orbital bias and high-spin vs low-spin bias. A reliable functional should have little or no bias of either type rather than succeeding for a limited subset of cases by cancellation of errors. We find that the widely used correlations of spin splittings to percentage of Hartree−Fock exchange are not borne out by the data, and the correlation functionals also play a significant role. We eventually conclude that SOGGA11-X, B1LYP, B3V5LYP, and MPW3LYP are the most consistently reliable functionals for balanced treatments of 4d transition metal atoms and their cations.

1. INTRODUCTION

Kohn−Sham density functional theory[1] and its generalizations to open-shell systems[2] and to orbital-dependent functionals[3] have been widely applied to transition metal chemistry, and they have been very successful and useful.[4] Nevertheless, if one were to generalize, one would have to say that the theory is not as accurate for typical transition metal systems as for main-group applications, so there is room for improvement. Since the theory is formally exact if one uses the unknown exact exchange−correlation (xc) functional, we seek improvement at the level of the xc functional, which is always approximate.

There are three specific issues that need to be considered in assessing the reliability of an xc functional for a transition metal complex: (i) Does it treat s and d subshells with comparable accuracy, or is it biased toward certain subshell occupancies? (ii) Does it treat high-spin and low-spin states with the same accuracy, or is it biased toward one or the other? (iii) Does it accurately balance localization on a single center (often leading to higher ionic character, higher spin state, or both) and delocalization across centers? Considerable information about these questions can be gleaned from molecular calculations, but there are advantages in studying them in atoms, too. The main advantages of atoms are the following: (a) Data on atomic energy levels are very complete and very accurate,[5] whereas molecular data are often missing for key compounds that would allow for systematic studies and when available often have large uncertainties. (b) Studying atoms allows us to study questions (i) and (ii) without the complication of question (iii) or the possible complication of systematic errors in molecular geometry, thereby disentangling some of the physics.

Motivated by these considerations, the present article reports a systematic study of the ability of approximate xc functionals to calculate energy levels in transition metal atoms, with a special emphasis on transitions involving a change in spin multiplicity or s and d occupancies or both. In particular, for each of the 4d transition metals in groups 3−10 of the periodic table, we study the lowest-energy multiplicity-changing transition in the neutral atom and its singly positive cation, as well as the adiabatic ionization potential. In 10 of the 16 cases (eight neutral atoms and eight cations), the lowest-energy multiplicity-changing transition involves a shift of electrons from an s orbital to a d orbital or vice versa (in four of these states the low-spin state has more s electrons than the high-spin state).

Our study will also consider the role of broken-symmetry solutions in the Kohn−Sham equations. It is well-known that the wave functions of systems with $n/2 > M_S$, where n is the number of unpaired electrons and M_S is the component of total electron spin (S) along the quantization axis, cannot be described properly by a single Slater determinant, and yet Kohn−Sham theory uses a single Slater determinant to represent the density. Therefore, for $M_S \leq S$, levels with $n > 2S$ cannot be treated in a natural way by Kohn−Sham theory. With the unknown exact xc functional, one would nevertheless get

Received: June 6, 2012
Published: August 27, 2012

   dx.doi.org/10.1021/ct300737t | J. Chem. Theory Comput. 2012, 8, 4112−4126

Table 1. Reference Data (After Removal of Spin−Orbit Coupling) from Experiments for All Excitation Energies and Ionization Potentials (in kcal/mol)

	Y	Zr	Nb	Mo	Tc	Ru	Rh	Pd
$\Delta E(M)^a$	31.27	13.93	−3.27	−30.79	−30.07	−18.71	−9.46	18.77
$\Delta E(M^+)^b$	2.40	−12.15	−15.90	−43.46	−9.90	26.16	−23.34	71.71
IP[c]	150.53	160.33	156.11	163.71	167.83	169.86	172.11	192.24

[a]The excitation energy of neutral atom, with the sign being positive if the lower energy state has a lower spin. [b]The excitation energy of the singly positive cation, with the same sign convention. [c]The ionization potential.

the correct energy and the correct density for the ground state, but the Kohn−Sham orbitals would not necessarily be spatial symmetry orbitals. Actually, they need not be symmetry orbitals even when $n/2$ is not greater than M_S, and currently available approximate density functionals often lead to a broken-spin-symmetry determinant. When $n/2 > M_S$, that broken-symmetry solution often seems to correspond to a mixture of two (or more) states with differing values of S (i.e., differing multiplicity). Interpreting the Kohn−Sham determinant as such a mixture of states allows one to approximate the correct spin state by performing two (or more) calculations with different M_S's and combining the results linearly with weights based on wave function theory;[6] we call this the weighted-average broken-symmetry (WABS) method. The WABS method has been very successful for transition metal complexes containing weakly coupled centers.[7] Extensions to strongly coupled cases (such as the states here where all orbitals are on the same center) have also been proposed.[8] Here we will explore the question of whether this method[8] provides general improvement over the straight variational approach.

We emphasize here that all the self-consistent-field (SCF) calculations presented in this paper were converged to a stable solution, meaning that the symmetry of spatial orbitals is allowed to be completely broken in the search for the lowest possible energy solution. Although useful insights might be obtained by careful analysis of the spatial orbitals of each spin state by restoring the spatial symmetry from the broken-symmetry solutions, this lies beyond the scope of the present work, which is intended to assess the qualities of various density functionals in describing 4d transition metal spin states in practical applications, where high spatial symmetry is usually not present.

We note that studies with some similarity to the present one have previously been carried out for p block elements[9] and for the 3d transition metals.[10] The former study included 56 density functionals for SCF calculations of multiplicity-changing excitations, and the latter included five density functionals.

Section 2 presents the experimental data to which we will compare. Section 3 specifies the xc functionals to be tested. Section 4 discusses the theory, computational methods, and basis sets. Section 5 contains the results and discussion, and section 6 consists of the conclusions.

2. EXPERIMENTAL DATA

Although the total electron spin quantum number S is not a good quantum number, we follow the usual Russell−Saunders labeling scheme in which atomic levels are labeled ^{2S+1}L, where L is the nominal total electronic angular momentum quantum number. For each element the two levels that we consider are the ground level and the lowest-energy level that has a different S.

The database for the present study is composed of all eight 4d transition metals in groups 3−10 of the periodic table, namely Y, Zr, Nb, Mo, Tc, Ru, Rh, and Pd. For each element the database contains the ionization potential (IP) and the lowest-energy multiplicity-changing excitation energy (ΔE) of both the neutral atom and its singly positive cation. Thus there are 24 data.

Scalar relativistic effects are included in the present calculations, but vector relativistic effects are not. Thus each level with a given L and S has degeneracy equal to $2S + 1$ or $2L + 1$, whichever is smaller. To obtain reference data for comparison with such calculations, we removed spin−orbit coupling (which is a vector relativistic effect) from the experimental data published in ref 5. We do this by taking advantage of the fact that the spin−orbit operator is traceless. Therefore it can be removed to first order by a degeneracy-weighted average:

$$\bar{E}(^{2S+1}L) = \frac{\sum_{J\ |L-S|}^{L+S} (2J+1)E(^{2S+1}L_J)}{\sum_{J\ |L-S|}^{L+S} (2J+1)} \quad (1)$$

where $^{2S+1}L_J$ denotes the state with total angular momentum J, and the left-hand side is the spin−orbit-free energy of the level. The energies resulting from applying eq 1 to the experimental data are shown as reference data in Table 1. Table 1 contains 16 ΔE's (eight for neutral atoms and eight for cations) and eight IPs. Since all 16 excitations considered here involve a change in S, we call one state the low-spin (LS) state and the other the high-spin (HS) state. All the ΔE's are calculated with the following sign convention:

$$\Delta E = E_{HS} - E_{LS} \quad (2)$$

3. DENSITY FUNCTIONALS

The exchange-correlation functional (xcF) is the quantity that must be approximated in the Kohn−Sham formalism.[1] Approximate xcFs can be categorized by considering the ingredients that they include. In their simplest form the xcFs only depend on the spin densities, ρ_σ, where σ is α or β, and such xcFs are known as local spin density approximations (LSDAs). When the reduced gradients, s_σ, of the spin densities are also used in the functionals, the functionals will be called gradient approximations. In most gradient approximations, called generalized gradient approximations (GGAs), the exchange part of the xcF has a separable form; if exchange is treated with a nonseparable form that also includes some correlation energy, the resulting functional is called a nonseparable gradient approximation (NGA). If the spin-labeled kinetic energy densities τ_σ (or the Laplacians of spin densities) are further introduced, the resulting xcFs are called meta-GGAs or meta-NGAs.

The energy densities of LSDAs, GGAs, NGAs, meta-GGAs, and meta-NGAs at a given spatial coordinate depend on functions (ρ_σ, s_σ, τ_σ) evaluated at that coordinate, and such functionals are called local functionals. On the other hand, the Hartree−Fock (HF) exchange energy density at a point in

Table 2. All the Density Functionals Tested in This Paper[a]

type	name	references
LSDA	GKSVWN3[b]	1, 11, 12
GGA	B88[c]	13
	BLYP	13, 14
	BP86	13, 15
	BPW91	13, 16
	HCTH/407	17, 18
	mPWLYP	14, 19
	OLYP	14, 20
	OPBE	20, 21
	PBE[d]	21
	PW91	16
	RPBE	22
	SOGGA	23
	SOGGA11	24
NGA	N12	25
global-hybrid GGA	B1LYP	26
	B3LYP	27
	B3LYP*	28
	B3PW91	29
	B3V5LYP	30
	B97-3	31
	B98	32
	BHandH	33
	BHandHLYP	33
	HFLYP[e]	14
	HFPW91[e]	16
	MOHLYP	34
	MPW1K	35
	MPW3LYP	36
	MPWB1K	37
	MPWLYP1M	34
	O3LYP	38
	PBE0[f]	39
	SOGGA11-X	40
range-separated hybrid GGA	CAM-B3LYP	41
	HSE	42, 43
	LC-mPWLYP[g]	44
	LC-ωPBE	45
	ωB97X	46
range-separated hybrid GGA-D	ωB97X-D	47
meta-GGA	M06-L	48
	M11-L	49
	revTPSS	50
	TPSS	51
	VS98[h]	52
meta-NGA	MN12-L	53
global-hybrid meta-GGA	BMK	54
	M05	55
	M05-2X	56
	M06	57
	M06-2X	57
	M06-HF	58
	M08-HX	59
	M08-SO	59
	MPWKCIS1K	19, 60, 61
	PW6B95	62
	TPSS1KCIS	50, 60, 64
	TPSSh	64
	τHCTHhyb	65
range-separated hybrid meta-GGA	M11	66

[a]Hartree−Fock is tested but not listed here. [b]Gáspár−Kohn−Sham for exchange and VWN3 for correlation (keyword SVWN in Gaussian). [c]Exchange functional with no correlation functional. [d]Also called PBEPBE. [e]Hartree−Fock exchange with correlation functional. [f]Also known as PBE1, PBE1PBE, or PBEh. [g]Obtained by applying Hirao's long-range correction[43] to the indicated GGA. [h]Also known as VSXC.

space depends on the integral of Kohn−Sham orbitals over the whole space, and by replacing a portion of local exchange with nonlocal Hartree−Fock exchange, one obtains a nonlocal functional. If the portion replaced is a constant percentage (i.e., a percentage independent of coordinates, ρ_σ, s_σ, τ_σ, or interelectronic separation), the resulting functional is called a global hybrid. Another way to include Hartree−Fock exchange is to partition the Coulomb operator into a short-range part and a long-range part, and treat one of them by local exchange and the other by Hartree−Fock exchange; xcFs constructed in this manner are called range-separated hybrid functionals. In some functionals, an empirical molecular mechanics term is added to the DFT energy to account for damped dispersion-like interactions. This kind of functional is called a DFT-D functional; if the molecular mechanics term is added to a GGA, it may be labeled GGA-D.

The Hartree−Fock approximation, although not an actual density functional method (and thus not shown in Table 2) is also included in this paper since it can be viewed as an approximate xcF, that is, as a pure-exchange density functional with no correlation and 100% Hartree−Fock exchange. The comparison of the Hartree−Fock method with functionals such as HFLYP (LYP correlation with 100% Hartree−Fock exchange) and HFPW91 (PW91 correlation with 100% Hartree−Fock exchange) allows for studying the effects of the correlation functional on the calculated excitation energies and IPs in a particularly transparent way.

We have in total tested 60 density functionals plus the Hartree−Fock method; the tested xcFs are listed in Table 2, each with one or more references.[11−66] There are one LSDA, 13 GGAs, one NGA, 19 global-hybrid GGAs, five range-separated hybrid GGAs, one range-separated hybrid GGA plus molecular mechanics dispersion (GGA-D), five meta-GGAs, one meta-NGA, 13 global-hybrid meta-GGAs, and one range-separated hybrid meta-GGA. The LSDA, the GGAs, the NGA, the meta-GGAs, and the meta-NGA are local; the hybrid functionals are nonlocal.

The specific considerations for choosing these density functionals were given a thorough discussion in a previous study of p block elements,[9] and we only point out here that several new functionals were added in the present work, most notably the new second order GGA family (SOGGA11[24] and SOGGA11-X[40]), the Minnesota 11 family (M11-L[49] and M11[66]), the recently proposed nonseparable functionals N12[25] and MN12-L,[53] and also the revTPSS[50] functional. SOGGA11 is the first GGA correct to second order in the density gradient that provides good accuracy for a broad variety of chemical problems; SOGGA11-X is the most successful global-hybrid GGA for calculations on a broad variety of chemical problems. M11 is the first range-separated meta-GGA, and it is optimized for a broad variety of chemical problems; it shows significant improvement over the (already very successful) previous generation of Minnesota functionals for

the databases examined in the article in which it is presented. M11-L is the first dual-range local meta-GGA and also the first local functional to have as good an average accuracy as hybrid functionals for many chemical properties. More importantly, it has good overall performance for multireference systems, which is expected to be a very important advantage for treating transition metals. The N12 functional is the first xcF depending only on the spin-labeled electron densities and their reduced gradients that simultaneously provides good accuracy for the four key energetic and structural properties of solids and molecules, namely, solid-state cohesive energies and lattice constants and molecular atomization energies and bond lengths. The MN12-L functional is a new local exchange-correlation energy functional that has significantly improved across-the-board performance, including main-group and transition metal chemistry and solid-state physics. The recent revTPSS functional is a revised version of the TPSS meta-GGA functional, constructed to be correct to the second order and to improve especially the lattice constants for solid-state calculations.

4. THEORY AND COMPUTATIONAL DETAILS

4.1. Theory. The WABS[6] method is briefly mentioned in section 1, and we shall discuss it in detail here. For all the ΔE calculations in this paper, the HS state is a state with $S = n/2$, where n is the number of unpaired electrons, whereas the LS state is a state with lower S. A state with $S = n/2$ can be well represented by a single Slater determinant with $M_S = n/2$, and thus it can be treated naturally by Kohn–Sham DFT. The LS state, however, often cannot be represented naturally by a single Slater determinant, and such states constitute particularly difficult cases for calculations with currently available approximate xcFs. In other cases we observe LS states that are treated well by a single Slater determinant; see section 5 for a detailed discussion. The unbalance of the accuracy expected for the many LS states that cannot be represented by a single Slater determinant as compared to the higher accuracy expected for HS states leads to systematic errors in calculated ΔEs since an accurate treatment of the excitation energy requires the LS and HS states to be described equally well.

If one does not fully optimize the Kohn–Sham Slater determinant, the results are sensitive to the choice of constraints imposed, and it is hard to impose the same kinds of constraints on molecules that one can impose in high-symmetry situations like atoms. Therefore, since our ultimate objective as chemists is accurate calculations on molecules, our first step in the solution of this problem is to allow the self-consistent-field process to break all the spatial symmetries in the calculations of both the HS and LS states, leading to the variationally lowest results one can possibly obtain. For the LS state, this yields the low-M_S broken-symmetry (BS) solution. There exist two strategies regarding how to utilize this stable solution:

(i) Use the low-M_S BS solution *as is*, and calculate the ΔE as the energy difference between the HS state and the low-M_S BS state.

(ii) Assume that the low-M_S BS state is a linear combination of the HS state and the actual LS state, and attempt to extract the energy of the LS state based on this assumption.

Strategy (i) will be called the variational method; it should work well if the LS state can be well represented by a single Slater determinant. However, this is often not true. In strategy (ii), which is the WABS method, the system is usually further classified into weakly coupled cases and strongly coupled cases.[7,8] The former usually involves two or more distant spin centers with weak coupling between the centers.[7] The atoms we study in this paper fall into the second type because (a) for a single atom there are no spin centers far apart in space and (b) the couplings between spins in different molecular orbitals of a single atom are usually much greater than the couplings between centers in binuclear or polynuclear transition metal complexes.

For the WABS calculations in this paper, we use the formula proposed by Yamaguchi[8]

$$\Delta E_{\mathrm{WABS}} = \frac{2S_{\mathrm{HS}}(E_{\mathrm{HS}} - E_{\mathrm{BS}})}{\langle \hat{S}^2 \rangle_{\mathrm{HS}} - \langle \hat{S}^2 \rangle_{\mathrm{BS}}} \tag{3}$$

(See the Appendix for a derivation.) Here S_{HS} is the total spin of the HS state, $\langle \hat{S}^2 \rangle_{\mathrm{HS}}$ and $\langle \hat{S}^2 \rangle_{\mathrm{BS}}$ are calculated expectation values of S^2, and BS denotes the low-M_S BS state. Equation 3 is based on the inference that a large spin contamination results from multideterminantal character of the actual LS state that leads to a significant mixing of the LS and HS states in the calculated BS state. Therefore, to extract the real excitation energies, the energy difference calculated from the gap between HS and BS states should be scaled by a factor proportional to the spin contamination. In contrast, for systems with little or no spin contamination in the calculated LS state, the BS solution should be used with strategy (i).

In practice we allow symmetry breaking in the HS state as well as the LS state so that all SCF calculations are converged to a stable solution. Thus the HS state may also have broken symmetry; in general, both the variational method and the WABS method involve broken-symmetry solutions. Again, we emphasize that this is consistent with the goal of the present work to test the qualities of xcFs in real-world transition metal chemistry applications, where high spatial symmetry is not present.

The s–d orbital transitions in 4d elements lead to complications in applying this method. First, some orbitals have mixed s and d character so there are noninteger occupations of s and d subshells in some states, and in these cases the spin contamination could originate from the partial occupations, from "pure" multireference character in d orbital configurations, or from both. WABS was originally formulated conceptually without considering noninteger subshell occupations, and we find that it can lead to little improvement or even worse results when orbitals are partially occupied. Furthermore, the spatial orbitals of the LS and HS states involving s–d transitions differ more than those without s–d transitions, which raises a concern as to whether the assumption of having the same orbitals in the two states is a safe assumption.

To clarify the questions above and to emphasize that complications in the spin states of transition metals should be analyzed on a case-by-case basis, in section 5.1 we separate the ΔE cases into ones involving large partial subshell occupations and those involving smaller or no partial subshell occupations and also into cases with and without s–d transitions. For each scenario we further compare the results with and without the use of WABS postprocessing.

4.2. Computational Details. All the density functional calculations were performed with a locally modified version of Gaussian 09.[67] For each state we performed a broken-symmetry calculation, using the spin-unrestricted formalism and not requiring symmetry orbitals. Furthermore, a stability test was carried out for each calculation, and the orbitals were optimized

Table 3. Comparison of Excitation Energies (in kcal/mol) Calculated with cc-pVTZ-DK and cc-pwcVTZ-DK Basis Sets

functional	Y	Y^+	Zr	Zr^+	Nb	Nb^+	Mo	Mo^+	Tc	Tc^+	Ru	Ru+	Rh	Rh^+	Pd	Pd^+
							cc-pVTZ-DK									
B3LYP	23.8	1.5	7.7	−7.4	−7.7	−14.2	−23.1	−28.3	−18.6	−5.5	−13.1	27.1	−5.5	−11.8	19.9	70.8
B88	13.1	−0.5	−4.8	−9.7	−18.9	−20.2	−36.1	−38.0	−32.9	−26.8	−22.9	5.2	−9.2	−13.3	11.1	55.7
HF	17.5	−4.5	0.3	−17.0	−16.7	−23.5	−33.3	−44.4	−23.3	−32	−17.0	8.4	−10.6	−18.9	−1.6	54.2
HSE	18.3	−2.0	−0.6	−10.6	−17.3	−19.5	−33.8	−35.1	−23.7	−12.4	−17.3	22.7	−7.9	−13.2	18.7	70.4
LC-ωPBE	19.0	−3.1	−1.0	−10.0	−18.2	−20.0	−29.5	−33.9	−21.4	−5.7	−16.3	28.9	−3.6	−11.8	23.5	77.6
M06	38.8	10.1	21.7	−6.9	5.5	−16.0	−8.0	−31.0	−15.4	1.0	−3.1	34.8	−0.6	−12.1	25.5	81.2
M06-L	28.6	6.1	13.7	−7.5	2.6	−12.9	−16.4	−28.8	−23.6	0.1	−11.4	37.6	−4.7	−16.9	21.1	76.1
ωB97X-D	29.3	0.4	13.4	−9.3	−3.1	−17.7	−15.5	−30.9	−17.0	−0.6	−7.1	35.3	−1.0	−11.1	26.1	80.6
PBE	17.9	−0.4	−0.6	−8.6	−14.5	−18.3	−30.0	−33.4	−24.1	−10.7	−15.9	23.0	−2.3	−11.7	21.9	71.4
SVWN	20.7	0.2	0.7	−9.7	−16.0	−20.5	−31.3	−35.1	−23.2	−9.7	−13.9	24.5	1.6	−9.8	26.9	77.1
							cc-pwcVTZ-DK									
B3LYP	23.8	1.5	7.6	−7.4	−7.7	−14.2	−23.1	−28.3	−18.6	−5.5	−13.1	27.1	−5.5	−11.8	19.9	70.8
B88	13.1	−0.5	−4.8	−9.7	−18.8	−20.2	−36.1	−38.0	−32.9	−26.8	−22.9	5.2	−9.2	−13.3	11.1	55.7
HF	17.4	−4.5	0.3	−17.1	−16.7	−23.5	−33.3	−44.2	−23.3	−32	−17.0	8.4	−10.6	−19.0	−1.6	54.2
HSE	18.2	−2.0	−0.6	−10.6	−17.3	−19.5	−33.8	−35.1	−23.8	−12.4	−17.3	22.6	−7.9	−13.2	18.7	70.4
LC-PBE	19.1	−3.1	−1.0	−10.1	−18.4	−20.1	−29.3	−33.9	−21.4	−5.7	−16.3	28.9	−3.6	−11.8	23.5	77.6
M06	38.8	10.0	21.6	−6.9	5.5	−16.0	−8.0	−31.0	−15.4	1.0	−3.1	34.8	−0.6	−12.1	25.5	81.0
M06L	28.6	6.1	13.9	−7.5	2.6	−12.9	−16.4	−28.8	−23.6	0.1	−11.4	37.5	−4.7	−16.9	21.1	76.1
ωB97X-D	29.5	0.4	13.4	−9.3	−3.1	−17.7	−15.5	−30.9	−17.0	−0.6	−7.1	35.3	−1.0	−11.1	26.1	80.6
PBE	17.9	−0.4	−0.6	−8.6	−14.5	−18.3	−30.1	−33.3	−24.0	−10.7	−15.9	23.0	−2.3	−11.7	21.9	71.4
SVWN	20.6	0.2	0.7	−9.7	−16.1	−20.5	−31.3	−35.1	−23.2	−9.7	−13.9	24.5	1.6	−9.8	27.0	77.3

(if instability was found) until the SCF solution was stable. For integrals over all space of the energy density, we used the "ultrafine" grid in the Gaussian 09 software; this is a pruned grid with 99 radial shells and 590 angular points in each shell. To calculate 5s and 4d subshell occupation numbers, natural bond orbital (NBO) analysis[68−75] was performed using the NBO 3.1 package with Gaussian 09. The scalar relativistic effect is included by using the Douglas−Kroll−Hess (DKH) second-order scalar relativistic Hamiltonian.[76−78]

We considered five all-electron basis sets specifically designed for DKH calculations of 4d elements. First we compared three triple-ζ basis sets: the cc-pVTZ-DK basis set of Petersen et al.[79] and basis sets by Hirao[80] and Huzinaga.[81] We carried out calculations for all three bases for a subset of the density functionals used in this paper, and we found that almost all the density functionals showed a reduced error compared to experiment when the cc-pVTZ-DK basis was used. Next, although one would expect core correlation effects to be less for 4d elements than for 3d ones, we tested the cc-pwCVTZ-DK[79] basis set, which includes 4s4p correlation, for a subset of 10 methods, in particular HF, SVWN, B88, PBE, B3LYP, LC-ωPBE, HSE, ωB97X-D, M06-L, and M06. Table 3 compares the results obtained from cc-pVTZ-DK and cc-pwCVTZ-DK calculations, showing that they agree within 0.2 kcal/mol. Finally, we considered the ANO basis of Roos et al.;[82] it is much larger than the cc-pVTZ-DK basis, but Petersen et al. found that it performs comparably to cc-pwCVTK-DK in CCSD(T) calculations. Therefore, the more manageable cc-pVTZ-DK basis was selected for our benchmark purposes, and all the remaining results reported here were obtained with the cc-pVTZ-DK basis set.

5. RESULTS AND DISCUSSION

5.1. 5s and 4d Subshell Occupations. The density functional calculations do not always yield integer occupancies for the 4d and 5s subshells because we always find variationally stable solutions, as mentioned above. Therefore we first consider the 5s subshell occupations. Tables 4 and 5 show, for each density functional and for Hartree−Fock theory, the mean signed deviation (called ε) and mean unsigned deviation (called δ) of the occupation number n_{5s} of the 5s subshell from the integer value characterizing the dominant determinant (according to the experimentally based tables of Moore[5]) for the 32 spin states we studied. (The 4d occupancy usually has an equal but oppositely signed error to that for the 5s, although in a few cases there is some small 5p occupancy of order 0.01.) We label the mean noninteger 5s occupancy as ε, and we label the mean absolute noninteger 5s occupancy as δ. Note that ε and δ should not necessarily be interpreted as errors because the exact Kohn−Sham orbitals need not be symmetry orbitals. Nevertheless, it is not clear whether presently available approximate density functionals might build in noninteger occupancies as a way to mimic configuration interaction effects of wave function theory or whether these noninteger occupancies should be viewed in a negative light. In the present work, our goal is to evaluate the functionals based on energetic comparison to experiment, and such comparisons do not suffer from such ambiguities. However, we will see that the noninteger occupancies are very helpful in understanding some of the results if we interpret a positive ε as a bias toward s orbitals and a negative ε as a bias toward d orbitals, so we shall use this interpretation.

Table 4 shows that 43 out of the 61 functionals have negative ε values for 5s occupancy, which implies an overstabilization of 4d orbitals relative to 5s. Furthermore, almost all of the 19 local functionals produce negative ε values, with the exceptions being B88, mPWLYP, and BLYP, which have small positive ε values of 0.01, 0.02, and 0.01. This is consistent with a previous study of 3d elements by Hirao et al.[10] Adding a small amount of Hartree−Fock exchange alleviates this bias, resulting in six global-hybrid GGAs with an ε that rounds to 0.00. This was also pointed out by a previous study,[83] which, however, was based on Slater exchange rather than Kohn−Sham exchange. Density functionals with a large percentage of Hartree−Fock exchange seem to overcorrect the bias of local functionals and are biased toward occupation of 5s orbitals, as most clearly observed in M05-2X, M06-2X, and BMK, but the bias is smaller than the bias in the other direction of the first 30 functionals in Table 4.

Table 4. Mean Noninteger Occupancy of the 5s Subshell Occupations for Each Method

functional	ε	functional	ε	functional	ε
N12	−0.17	MOHLYP	−0.05	M08-SO	−0.01
MN12-L	−0.16	PBE	−0.05	M06-HF	0.00
OPBE	−0.14	PW91	−0.05	B3V5LYP	0.00
PW6B95	−0.13	MPW1K	−0.05	B3LYP*	0.00
SOGGA11	−0.11	M11	−0.05	B3LYP	0.00
MPWB1K	−0.10	M05	−0.04	LC-mPWLYP	0.00
M11-L	−0.10	M06	−0.04	MPW3LYP	0.00
OLYP	−0.09	HFLYP	−0.04	SOGGA11-X	0.00
O3LYP	−0.08	BP86	−0.04	BHandHLYP	0.00
TPSS	−0.08	M06-L	−0.03	MPWLYP1M	0.01
revTPSS	−0.08	τHCTHhyb	−0.03	B88	0.01
LC-ωPBE	−0.07	HSE	−0.03	CAM-B3LYP	0.01
TPSSh	−0.07	GKSVWN3	−0.03	BLYP	0.01
BPW91	−0.07	M08-HX	−0.03	BHandH	0.01
HCTH/407	−0.07	B98	−0.02	B1LYP	0.01
TPSS1KCIS	−0.06	VS98	−0.02	M06-2X	0.02
B3PW91	−0.06	ωB97X	−0.02	BMK	0.02
RPBE	−0.06	MPWKCIS1K	−0.02	mPWLYP	0.02
HFPW91	−0.06	ωB97XD	−0.01	M05-2X	0.03
SOGGA	−0.06	B97-3	−0.01		
PBE0	−0.05	HF	−0.01		

Whereas Table 4 has the functionals in order of increasing ε, Table 5 has them in order of increasing δ. The result is that almost all the entries in the first half (31) of the 61 entries of Table 5 are hybrid functionals, with the only exception being VS98, which is in position 26 with an ε of 0.08. It is also notable that the pure Hartree−Fock exchange functional is positioned near the very bottom of the ordered list. These observations confirm the conventional wisdom that an appropriate amount of Hartree−Fock exchange for an unbiased description of the 5s and 4d orbitals is neither 0 nor 100%.

Whereas Tables 4 and 5 show averages of the noninteger 5s occupancies over spin states for each functional, Table 6 shows averages of the noninteger 5s occupancies as averaged over all functionals for each of the 32 spin states. Table 6 also shows the experimental multiplicity $2S + 1$ and experimental 5s occupation numbers. We find that, for a given spin state, all the methods tend to produce errors in the 5s occupancies with the same sign (either positive or negative). The results show that there are six spin states (in italic type) with an ε more negative than −0.10, implying a strong bias toward occupation of 4d orbitals, and there are two states (in boldface type) with an ε more positive than 0.10, implying a strong bias toward occupation of 5s orbitals. The 5s/4d occupations are more properly described in the remaining 23 spin states.

We should be careful to distinguish *actual 5s occupancy* (an output variable obtained by NBO analysis of the orbitals) from *nominal 5s occupancy change* (an input variable, as part of the initial guesses for the HS and LS SCF processes, based on the dominant configurations of the experimental states). In addition to the *deviation from an integer* of the actual in 5s occupancy *in each of the 32 spin states* involved in the multiplicity-changing transitions, it is also important to consider *changes* in the nominal 5s occupancy *in each of the 16 transitions*. By taking into account both considerations, we divide the 16 ΔE cases into four groups:

In *group 1*, neither the LS nor the HS state has a large-magnitude ε, and there is no change in nominal s and d occupancies involved in the excitation. This group contains the ΔE's of Mo, Mo^+, Ru, and Rh^+. In all these cases it turns out that $\langle \hat{S}^2 \rangle$ for the low-M_S BS state is close to what one expects for a 50:50 mixture of the HS and LS states; that is, there is large spin contamination. For the 4d transition metals in this study, we did not find any cases involving a change in nominal 5s occupancy that had a small error in the 5s occupancies of both the HS and LS states but large spin contamination (although this does occur for some other transition metals).

In *group 2*, neither the LS nor the HS state has a large-magnitude ε, but the multiplicity-changing excitation does involve a nominal s−d transition. This group contains Y, Tc^+, Ru^+, Pd, and Pd^+. In these cases it turned out that the $\langle \hat{S}^2 \rangle$ values are close to those for pure spin states.

Table 5. Mean Unsigned Deviation (δ) of 5s Subshell Occupations from That of the Dominant Experimental Configuration

functional	δ	functional	δ	functional	δ
BMK	0.02	B3LYP*	0.07	M11-L	0.12
ωB97X-D	0.03	B3LYP	0.07	MOHLYP	0.13
LC-mPWLYP	0.03	M08-HX	0.07	TPSSh	0.13
SOGGA11-X	0.03	M11	0.07	RPBE	0.13
BHandH	0.03	VS98	0.08	SOGGA	0.13
BHandHLYP	0.03	HSE	0.08	MPWB1K	0.13
ωB97X	0.04	HFPW91	0.08	HCTH/407	0.13
CAM-B3LYP	0.04	M06-HF	0.09	BPW91	0.14
M08-SO	0.04	MPWLYP1M	0.09	OLYP	0.14
M05-2X	0.05	mPWLYP	0.09	SOGGA11	0.14
B97-3	0.05	BLYP	0.09	M06-L	0.15
B98	0.05	MPW1K	0.09	revTPSS	0.15
HFLYP	0.05	PBE0	0.1	HF	0.16
MPWKCIS1K	0.05	B3PW91	0.11	TPSS	0.16
B1LYP	0.05	LC-ωPBE	0.11	B88	0.17
M05	0.06	GKSVWN3	0.11	PW6B95	0.17
M06	0.06	TPSS1KCIS	0.12	OPBE	0.19
τHCTHhyb	0.06	PBE	0.12	N12	0.20
B3V5LYP	0.06	PW91	0.12	MN12-L	0.24
MPW3LYP	0.06	O3LYP	0.12		
M06-2X	0.07	BP86	0.12		

dx.doi.org/10.1021/ct300737t | J. Chem. Theory Comput. 2012, 8, 4112−4126

Table 6. Multiplicity, 5s Subshell Occupancies, and ϵ for Each Level[a]

	Y		Y^+		Zr		Zr^+	
multiplicity	2	4	*1*	3	3	5	*2*	*4*
exptl n_{5s}	2	1	*2*	1	*2*	1	*1*	*1*
ϵ	−0.08	−0.02	*−0.54*	−0.05	*−0.12*	−0.03	*−0.14*	*−0.21*
	Nb		Nb^+		Mo		Mo^+	
multiplicity	*4*	*6*	**3**	5	5	7	4	6
exptl n_{5s}	*2*	1	**0**	0	1	1	0	0
ϵ	*−0.29*	−0.02	**0.26**	0.10	0.05	−0.03	0.04	0.00
	Tc		Tc^+		Ru		Ru^+	
multiplicity	4	*6*	5	7	3	5	4	6
exptl n_{5s}	1	*2*	0	1	1	1	0	1
ϵ	0.01	*−0.46*	0.07	−0.03	−0.07	0.02	0.00	0.00
	Rh		Rh^+		Pd		Pd^+	
multiplicity	**2**	4	1	3	1	3	2	4
exptl n_{5s}	**0**	1	0	0	0	1	0	1
ϵ	**0.30**	0.00	0.00	0.00	0.00	0.00	0.00	0.00

[a] n_{5s} is the occupancy of the 5s subshell, and ϵ is the mean signed deviation, averaged over the 59 calculations of that occupancy, from the integer value that characterizes the configuration that is experimentally found to be dominant

In *group 3*, one of the two states suffers from a large-magnitude ϵ. We find that all such cases also happen to involve a nominal s−d transition. This group contains Y^+, Zr, Nb, Tc, and Rh.

In *group 4*, both the LS and HS states have a large-magnitude ϵ. This group contains only Zr^+ and Nb^+, and neither of them involves a nominal s−d transition.

Next, results for these four groups will be discussed separately, after which a brief summary and further discussion will be provided. Finally, we will discuss the overall performance of the functionals and methods and make recommendations.

5.2. Group 1 Cases. Since all the spin states in this group present neither nonintegral subshell occupation nor s−d transitions, group 1 cases are the most "pure" ones for discussing the performance of density functionals for spin states and the usefulness of WABS methods. The results are presented in Table 7, with the four columns of numbers corresponding to the MSEs and MUEs before and after WABS treatment, where MSE is the mean signed error in ΔE and MUE is the mean unsigned error in ΔE.

A first observation is that before postprocessing with the WABS treatment, i.e., employing the variationally stable states without reinterpretation by the WABS method, all the methods overestimate ΔE, resulting in a positive MSE value. Also we find (not shown) that all the LS states have a calculated $\langle \hat{S}^2 \rangle$ close to the one of a state with a half-and-half linear combination of the HS and the LS states. Since for group 1 all the experimental ΔE values are negative (meaning the LS state is higher than the HS one), this puts the broken-symmetry low-M_S variational solution halfway between the HS state and the actual LS state and results in a *less negative* excitation energy; this explains the positive MSE. Furthermore, there is no fractional s occupancy in either of the spin states involved in the transition, and the LS and the HS states tend to have very similar spatial orbitals. This then is precisely the situation that the WABS postprocessing method was originally designed to treat.

After WABS treatment, the MSEs for various functionals have both positive and negative values, and the MUE values are usually improved, as shown in the fifth and tenth columns of Table 7. In fact, in 54 cases the MUE is lowered, in one case (M11-L) it stays the same, and in only four cases (MPW1K, HFPW91, B88, and HF) it increases. For group 1, then, the errors remaining after WABS treatment may be considered to be the "pure" spin-coupling errors of the corresponding density functionals, independent of whether they have a bias toward s or d occupancy, and we find the best functional to be O3LYP with an MUE of 1.9 kcal/mol. This is consistent with a previous finding that O3LYP performs well in spin-state calculations.[9] Only slightly less accurate are MOHLYP, BP86, MPWB1K, and PW6B95.

It is usually said that Hartree−Fock theory has a bias toward HS states and local density functionals have a bias toward LS states. The former can be rationalized by the fact that HF theory includes the Fermi hole but not the Coulomb hole; the latter can be rationalized by the fact that local functionals do not cancel self-interaction errors. The results in Table 7 are only partly consistent with this. HF does have a large negative ΔE as does HFPW91, but HFLYP has a positive MSE. This shows the important role of correlation energy changes in spin-flip transitions. Furthermore, Table 7 shows little correlation between the percentage of HF exchange and the sign of MSE.

To summarize, we find that much of the systematic error in ΔE for group 1 species originates from the multideterminantal character of the LS state. Since the LS and HS states tend to have similar spatial orbitals, the WABS postprocessing treatment significantly improves the results. Comparison of the resulting excitation energies to experiment, as summarized in the WABS columns of in Table 7, reveals which functionals are well balanced in their treatment of different multiplicites.

5.3. Group 2 Cases. In transition metal chemistry the simple situation discussed in section 5.2 is commonly complicated by the possible overstabilization of s or d orbitals, which leads to partial

Table 7. MSE and MUE of ΔE for Group 1 by the Variational and WABS Methods

	var		WABS			var		WABS	
functional	MSE	MUE	MSE	MUE	functional	MSE	MUE	MSE	MUE
O3LYP	8.1	8.1	0.4	1.9	revTPSS	6.0	6.2	−2.4	4.8
MOHLYP	9.2	9.2	2.1	2.1	B3PW91	4.0	6.0	−4.6	4.9
BP86	8.2	8.2	0.8	2.1	MPWLYP1M	11.4	11.4	4.9	4.9
MPWB1K	8.3	8.3	0.7	2.2	TPSS1KCIS	5.7	6.5	−2.6	5.1
PW6B95	9.3	9.3	2.2	2.2	MPW1K	3.8	5.0	−5.2	5.2
LC-ωPBE	6.2	6.2	−1.7	2.3	OPBE	3.6	5.3	−5.2	5.2
RPBE	7.1	7.1	−0.7	2.3	HFPW91	4.2	4.2	−5.3	5.3
OLYP	8.8	8.8	1.4	2.3	mPWLYP	11.7	11.7	5.3	5.3
PBE	6.3	6.3	−1.6	2.4	BHandHLYP	10.8	10.8	3.6	5.5
PW91	6.6	6.6	−1.2	2.4	BMK	11.8	11.8	5.8	5.8
BPW91	6.1	6.1	−1.9	2.8	B97-3	12.3	12.3	6.1	6.1
GKSVWN3	6.6	6.8	−0.8	2.8	B98	12.7	12.7	6.5	6.5
B3LYP*	9.9	9.9	2.9	2.9	M08-HX	11.2	11.2	4.9	6.6
M08-SO	9.0	9.0	2.3	3.0	ωB97X-D	12.9	12.9	6.9	6.9
B3V5LYP	10	10	3.0	3.2	HCTH/407	11.6	11.6	4.8	6.9
B3LYP	10	10	3.0	3.2	VS98	9.1	9.1	1.6	7.2
BHandH	9.2	9.2	1.9	3.3	LC-mPWLYP	13.2	13.2	7.4	7.4
MPWKCIS1K	6.6	6.6	−1.6	3.5	B88	1.5	6.3	−7.9	7.9
SOGGA	4.6	5.8	−3.7	3.7	M06-L	10.7	10.7	2.9	8.2
SOGGA11-X	9.8	9.8	2.8	3.8	HFLYP	11.1	11.1	3.5	8.3
MPW3LYP	10.6	10.6	3.8	3.9	τHCTHhyb	14.2	14.2	8.4	8.4
TPSS	6.8	6.8	−1.2	4.0	HF	0.7	2.4	−10	10.0
SOGGA11	10.5	10.5	4.2	4.2	MN12-L	13.8	13.8	7.2	10.1
M11	5.2	5.2	−2.7	4.2	M06	15.5	15.5	9.9	10.3
B1LYP	10.6	10.6	3.7	4.3	M11-L	11.7	11.7	3.7	11.7
PBE0	4.2	5.6	−4.4	4.4	M05-2X	17.0	17.0	12.3	12.3
HSE	4.2	5.7	−4.4	4.4	ωB97X	17.6	17.6	12.7	12.7
N12	9.2	9.2	2.6	4.4	M05	18.8	18.8	14.1	14.1
CAM-B3LYP	11.2	11.2	4.6	4.6	M06-2X	18.5	18.5	14.1	14.1
BLYP	11.2	11.2	4.6	4.6	M06-HF	18.8	18.8	14.1	14.1
TPSSh	5.8	5.9	−2.6	4.8					

occupations through hybridization. This could accidently favor either the LS or the HS state on a case-by-case basis. The entanglement of these effects, bias toward high S or low S and bias toward high s:d or low s:d, usually results in complex and hard-to-interpret scenarios. However, group 2 species provide relatively clear cases in the sense that we find that both spin contaminations and nonintegral subshell occupation numbers are negligible for almost all methods in both states of each transition. The former seems to indicate that both the LS and the HS states are single-reference ones, and the latter means that the 5s and 4d orbitals are treated without the complication of hybridization.

Table 8 presents the calculated MSEs and MUEs of all the functionals for the group 2 excitation energies. Since a small amount of spin contamination exists for certain functionals in certain states, we also report in the fourth and eighth columns in Table 8 the MUEs after WABS postprocessing. However, the comparison to the unprocessed results shows that the improvement by WABS is less than 2 kcal/mol, and for many cases the error increased after WABS treatment. Furthermore, in group 2 the $\langle \hat{S}^2 \rangle$ values are close to those for pure spin states, so the deviation from the pure-state values need not be dominated by a simple mixing of two states. Therefore, we do not recommend WABS corrections for group 2 calculations, and all the discussions of group 2, except where indicated otherwise, will be based on the variational results.

An MSE of −18.3 kcal/mol for Hartree−Fock theory implies a strong favoring of the HS state, which is consistent with the common expectation. If one compares the local functionals with their hybrid counterparts, however, the results are mixed. For most cases, an increased (although only by a small amount) favoring of the HS state is observed when the percentage X of Hartree−Fock exchange is raised, such as PBE vs PBE0, PW91 vs HFPW91, and BLYP vs HFLYP. The same effect is also seen for OLYP vs O3LYP and MPWLYP vs MPW3LYP, even though the correlation functional changes a little when X is raised in these cases. We also see apparent exceptions such as SOGGA11 vs SOGGA11-X and M06-L vs M06 vs M06-2X; we note, though, that in these cases the local part is reoptimized significantly when X is changed.

Now turn to MUEs of the excitation energies. We find the top 10 and most of the top half of the list are hybrid functionals, with the best being BHandH with 50% Hartree−Fock exchange. The best local functional for group 2 is BLYP with an MUE of 3.6 kcal/mol, and most local functionals are ranked near the bottom with an MUE larger than 5 kcal/mol. This is in contrast with group 1, where, after WABS correction, the top 10 contains five local functionals and five hybrid functionals. Furthermore, no density functional appears in the top 10 density functionals of both groups. If, however, we had included WABS postprocessing for group 2, MPWB1K, BP86, and RPBE would be in the top 10 for both groups.

The large differences that we find in functional rankings between group 1, which does not involve an s−d transition, and group 2, which does involve an s−d transition, seem to imply

Table 8. MSE and MUE of ΔE for the Variational Method and MUE of ΔE for the WABS Method for Group 2

	var		WABS		var		WABS
functional	MSE	MUE	MUE	functional	MSE	MUE	MUE
BHandH	−1.6	1.6	1.7	LC-mPWLYP	4.0	4.8	6.0
BMK	1.6	2.4	3.5	VS98	1.9	4.9	3.5
MPWKCIS1K	−2.1	2.6	1.0	M06-HF	5.0	5.0	8.6
MPW3LYP	−0.2	2.7	2.0	MOHLYP	1.3	5.1	3.3
B3V5LYP	−0.6	2.8	1.6	GKSVWN3	0.3	5.2	3.7
B1LYP	−0.7	2.8	1.9	M08-SO	3.0	5.6	7.8
B3LYP*	−0.4	3.0	1.6	SOGGA	−3.7	5.7	4.4
B3LYP	−0.4	3.0	1.7	LC-ωPBE	1.1	6.0	4.5
CAM-B3LYP	1.2	3.1	3.1	M06-L	5.1	6.2	7.1
BHandHLYP	−1.0	3.1	2.8	B97-3	5.4	6.5	7.5
SOGGA11-X	2.9	3.2	5.0	B98	5.6	6.7	7.6
TPSS1KCIS	−1.4	3.3	1.5	O3LYP	2.6	7.1	5.3
MPWLYP1M	0.0	3.3	2.5	ωB97X-D	6.5	7.3	8.5
mPWLYP	0.1	3.5	2.6	M08-HX	7.6	7.8	9.7
BLYP	−0.3	3.6	2.1	OPBE	0.5	8.0	6.3
MPWB1K	0.1	3.6	2.0	OLYP	3.4	8.1	6.1
PBE0	−3.4	3.7	2.3	SOGGA11	2.9	8.1	6.4
PW6B95	0.9	3.7	2.6	τHCTHhyb	8.3	8.3	10.5
B3PW91	−3.2	3.8	2.5	HCTH/407	8.4	8.4	11.6
MPW1K	−3.8	3.8	2.4	MN12-L	4.7	8.6	11.1
BP86	−2.1	3.8	2.0	M06	8.7	8.7	11.3
TPSSh	−2.1	3.9	2.2	M06-2X	9.0	9.0	11.7
RPBE	−2.1	3.9	2.0	M11	5.3	9.5	8.1
HFLYP	−1.2	3.9	4.8	N12	4.1	10.2	9.7
HSE	−4.1	4.1	2.6	ωB97X	11.3	11.3	13.9
PBE	−2.9	4.2	2.7	M05-2X	11.4	11.4	14.1
PW91	−2.9	4.2	2.7	M11-L	11.4	13.0	13.6
revTPSS	−2.3	4.2	2.5	M05	14.7	14.7	17.1
HFPW91	−3.6	4.3	2.9	B88	−15.9	15.9	15.0
TPSS	−2.0	4.3	2.5	HF	−18.3	18.3	17.1
BPW91	−3.7	4.8	3.5				

that excitations with and without s−d transitions are of distinctive character, and this should be carefully considered in assessing the quality of density functionals and in constructing representative subsets of 4d elements.

The conclusion that excitations with and without s−d transitions have different characters has profound implications for the many studies of multiplicity-changing transitions in polyatomic molecules. In molecules there is a continuum of s−d mixing due to changes in hybridization, and the hybridization state may change more or less upon a multiplicity-changing excitation, but in general the past attempts to draw conclusions about the accuracies of various functionals for multiplicity-changing transitions have not taken this into account.

5.4. Group 3 Cases. Now we turn to the more problematic group 3 cases, in which the 5s subshell has a noninteger occupation in either the LS or the HS state. We note that each calculated LS state in group 3, except that of Tc, suffers from a fair amount of spin contamination, but the calculated $\langle \hat{S}^2 \rangle$ value is still far from the one of a half-and-half linear combination of the HS and the LS states, and unlike group 1, the spin contamination values in group 3 depend heavily on the density functional being used. One should note there are actually two sources of spin contaminations for transition metals: (i) partial occupations of s or d orbitals and (ii) multideterminantal character in representing the electron configurations in the five d orbitals when $n/2 > M_S$. Furthermore, in complicated cases these two sources can be in effect at the same time. Spin contaminations from group 1 arise only from source (ii) since there is no partial occupation, and group 1 is most suitable for WABS treatment because the spatial orbitals of the LS and HS states are potentially very similar. In contrast, spin contaminations of LS states in group 3 mostly originate from source (ii), as revealed by Figure 1, where we plot the absolute error in $\langle \hat{S}^2 \rangle$ against δ for Y^+, Zr, Nb, and Rh and find a nearly linear dependence in all four cases; Tc is not plotted because for that case it is the HS state that has partial occupations and the spin contaminations for all functionals turn out to be negligible for Tc.

In the WABS method employing eq 3, the spin contamination is used as a sign of multiconfiguration character in the BS state, and it is utilized to scale the LS−HS gap proportionally, but this is only valid if the orbitals are the same (or almost the same) in the HS and BS solutions. This is usually achieved only if no noninteger occupation of subshells is involved. The multiplicity-changing excitations in group 3 species all happen to involve an s−d transition, and just like group 2, the orbitals in the LS and HS states tend to differ more in this circumstance. In addition, one state has noninteger 4s occupancies and the other does not. For these reasons one would not expect WABS postprocessing to offer meaningful improvement for ΔE values for group 3, and yet Table 9 does show improvement in MUE for most of the functionals, although it is usually less than 1 kcal/mol, and the errors even increase for some functionals. Additionally, the MUE in general increases as δ increases, which again is consistent with our

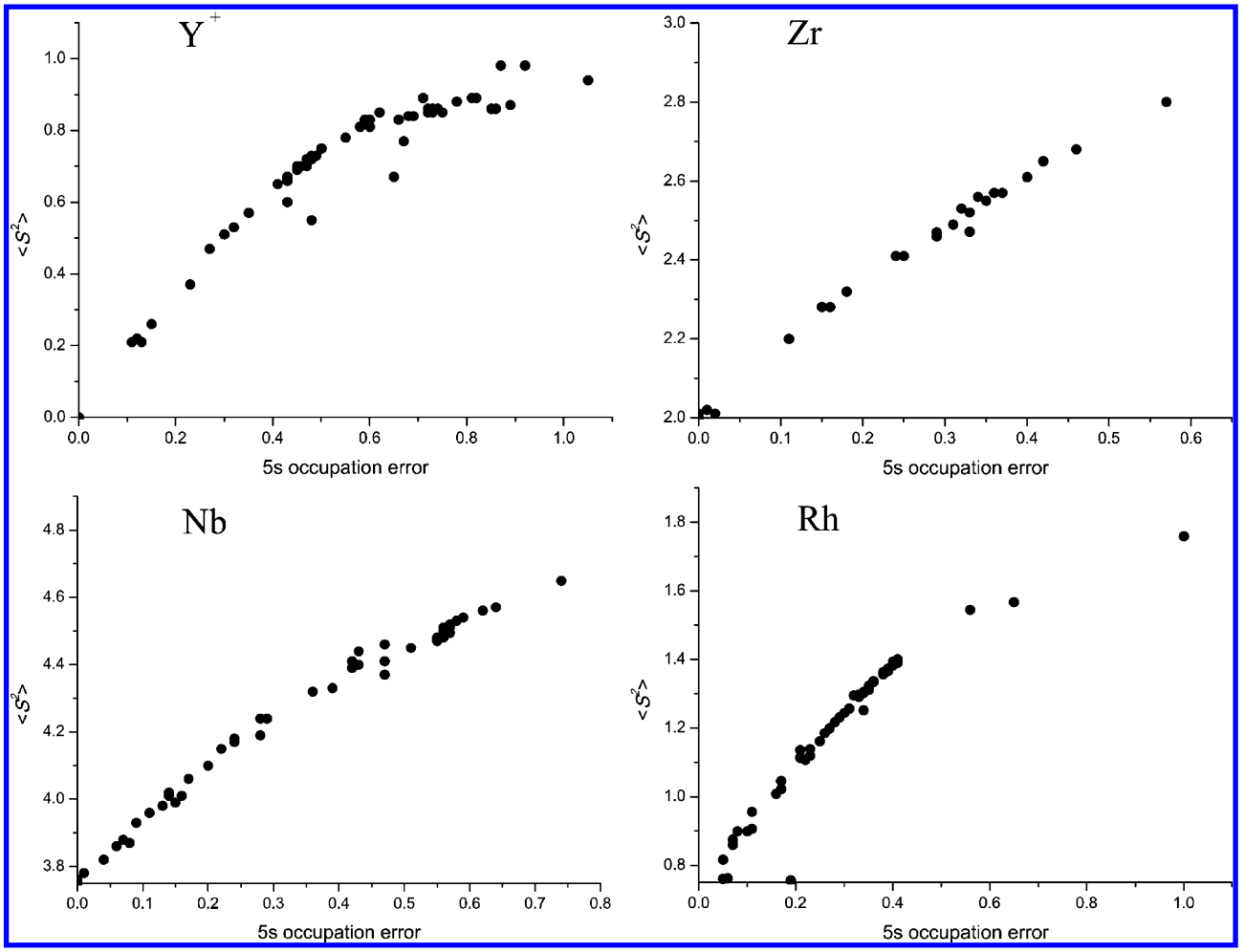

Figure 1. Plots of calculated $\langle \hat{S}^2 \rangle$ values against the absolute error in 5s subshell occupations for Y^+, Zr, Nb, and Rh.

conclusion that the main error in group 3 atoms and cations results from nonintger subshell occupations.

If we look at the MUEs either before or after WABS postprocessing, the best performing functional either way is SOGGA11-X with an error of 2.2 kcal/mol before and 1.6 kcal/mol after. If we order the functionals based on MUE after the WABS treatment, then 19 of the best 20 density functionals are hybrid functionals, with the only exception being M06-L with an MUE of 3.8 kcal/mol. Again using the WABS MUE, three functionals in the top 10 for group 3 are also found in the best 10 for group 2, namely, BHandH, BMK, and B1LYP, which could be due to the fact that group 2 and group 3 excitations both involve s−d transitions, and thus they share a common characteristic. However, as in group 2, there is no overlap between the best 10 for group 3 and the best 10 for group 1.

5.5. Group 4 Cases. Group 4 only includes Zr^+ and Nb^+, for which we found that the broken-symmetry solutions of both the LS and the HS states present high spin contamination. Furthermore, the calculated $\langle \hat{S}^2 \rangle$ values are very close to the ones for a half-and-half linear combination of the LS and the HS states, which is very similar to group 1. This seems to imply that results would be improved after applying WABS postprocessing. However, when one compares the calculated MUEs before and after WABS postprocessing in Table 10, we see that for more than 40 functionals the averaging procedure deteriorates the accuracy. Also note that no nominal s−d transition is involved in either cation, excluding possible impacts from this aspect. Thus if we compare group 1 and group 4, the main difference is the noninteger occupations of s and d subshells. Consequently, a possible explanation for the poor performance of WABS seems to be that the orbitals of the LS and HS states differ significantly from each other, and this contradicts the underlying assumptions of the WABS method.

Next, we will discuss the MSE and MUE results of the variational calculations for group 4. First consider MSEs. The largest negative MSE is −6.2 kcal/mol for HF and is again consistent with the common conclusion that HF is biased toward the HS state. Also, we find that most density functionals favor the LS state (i.e., they have a positive MSE). If one focuses on the MUE of each functional, then—surprisingly—HFLYP, a simple hybrid GGA with 100% HF exchange, is the best performing functional with an MUE of merely 0.7 kcal/mol. This seems to be mainly due to its very small ε of 0.03. In general the absolute errors appear to decrease as ε decreases, but this is not as evident as in group 3 (where only one state has noninteger subshell occupation), especially when we notice that, in the best 10 functionals, five, namely TPSSh, revTPSS, B98, ωB97X, and TPSS, have ε greater than or equal to 0.19.

We conclude that the situations for the group 4 species are too complicated for a general interpretation, and they serve as typical examples where multireference character (suggested by a very large spin contamination) is not properly treated by averaging due to having very different orbitals of the LS and the HS states. Although the key factor in improving the accuracy

dx.doi.org/10.1021/ct300737t | J. Chem. Theory Comput. 2012, 8, 4112−4126

Table 9. MSE and MUE of ΔE for the Variational Method, MUE of ΔE for the WABS Method, and δ of the 5s Subshell Occupation for Group 3

	var		WABS	var		var		WABS	var
functional	MSE	MUE	MUE	δ^a	functional	MSE	MUE	MUE	δ^a
SOGGA11-X	2.2	2.2	1.6	0.03	MPWKCIS1K	−3.8	7.3	7.0	0.15
BMK	3.0	3.0	1.8	0.06	O3LYP	0.0	7.4	6.9	0.41
BHandH	−0.6	3.1	2.1	0.05	TPSS1KCIS	−2.6	7.4	6.4	0.47
BHandHLYP	0.2	3.3	2.5	0.06	BP86	−1.6	7.5	6.6	0.41
HCTH/407	4.2	4.2	5.2	0.21	HFLYP	1.6	7.6	7.3	0.22
M06-L	4.1	4.2	3.8	0.43	RPBE	−2.0	7.7	6.8	0.44
B98	3.8	4.3	3.6	0.11	OLYP	1.0	7.8	7.7	0.45
LC-mPWLYP	3.4	4.3	3.3	0.05	B88	−8.0	8.1	11.2	0.45
M08-SO	2.3	4.4	5.7	0.08	PBE0	−4.7	8.2	7.5	0.38
B1LYP	1.2	4.4	3.1	0.09	HSE	−5.0	8.2	7.3	0.31
B97-3	3.9	4.5	3.9	0.14	PW91	−2.9	8.2	7.5	0.42
CAM-B3LYP	1.9	4.6	3.4	0.08	B3PW91	−4.8	8.3	8.0	0.42
MPW3LYP	1.4	4.6	3.6	0.13	PBE	−3.1	8.3	7.6	0.42
ωB97X-D	3.8	4.8	4.0	0.10	HF	−5.7	8.4	8.8	0.40
B3V5LYP	0.8	5.2	4.0	0.18	M05-2X	8.8	8.8	9.4	0.10
MPWB1K	−1.2	5.3	4.2	0.07	MPW1K	−6.2	8.9	8.9	0.35
MPWLYP1M	2.4	5.4	4.8	0.21	M11	0.4	8.9	7.5	0.23
B3LYP	0.8	5.4	4.1	0.19	BPW91	−3.9	9.1	8.7	0.48
MN12-L	5.2	5.2	4.2	0.17	M06-2X	9.2	9.2	9.6	0.18
B3LYP*	0.8	5.7	4.6	0.21	GKSVWN3	−2.0	9.2	8.6	0.29
mPWLYP	2.5	5.7	5.2	0.20	SOGGA	−4.5	9.3	9.7	0.44
PW6B95	0.2	5.7	4.7	0.09	ωB97X	9.4	9.4	8.7	0.03
τHCTHhyb	5.8	5.8	5.1	0.11	M06	9.6	9.6	8.8	0.14
BLYP	1.7	6.0	5.4	0.24	LC-ωPBE	−4.2	10.0	9.7	0.39
VS98	0.2	6.7	5.9	0.15	OPBE	−3.9	10.2	10.4	0.56
M08-HX	3.2	6.7	6.4	0.18	M05	10.7	10.7	10.1	0.10
MOHLYP	1.5	6.8	6.6	0.40	HFPW91	−6.7	10.7	11.0	0.27
revTPSS	−3.0	6.9	5.9	0.44	SOGGA11	−0.4	10.7	10.6	0.47
TPSSh	−3.4	7.0	6.1	0.44	N12	−3.9	12.7	12.4	0.35
M11-L	4.2	7.1	6.4	0.41	M06-HF	11.9	11.9	14.0	0.27
TPSS	−2.6	7.3	6.3	0.45					

[a] δ denotes the mean unsigned deviation of the 10 occupancies in group 3 of the 5s subshell from the integer values corresponding to the dominant configuration of the experimental state.

seems to be connected with a proper description of s and d orbitals to eliminate partial occupations, this is not as conclusive as in group 3. In general, one should consider the best functionals in this group to be achieving their success or partial success fortuitously, and it is recommended to not include this group in assessment or design of functionals for transition metals due to the entanglement of several effects.

5.6. Overall Performance. We shall briefly summarize our observations here, with an attempt to gain some insights for an appropriate assessment of the overall performance of all the methods.

Group 1 contains the clearest cases of where WABS post-processing can help because the error is dominated by multi-determinental character of the LS states. Since WABS post-processing significantly improves the accuracy of almost all functionals, we conclude that only WABS-corrected results should be used to assess the intrinsic error of each functional for spin states in this group. Group 2 and group 3 share some similarities in that both involve s−d transitions in multiplicity-changing excitations. The former group has little spin contamination, and all of its states are single-reference ones. The spin contaminations of group 3, although non-negligible, are smaller than those for group 1 and, as distinct from group 1, seem to result mainly from noninteger subshell occupations. WABS postprocessing improves the results very little for groups 2 and 3 and also generally does not change the trends of the results. Therefore we use the variational results for these groups for the final analysis. Group 4 has large spin contaminations for LS states, but WABS postprocessing worsens the results; also, most functionals working well in this group should be considered to be working by fortuitous cancellation of errors. This leads us to exclude this group from our final assessment, and further leads to a database of 28 states, with 14 ΔE's and 8 IPs.

Another important observation is that the noninteger subshell occupations tend to be closely associated with the energy errors. In groups 1 and 2, only small partial occupations are observed so all the functionals are assessed equally. In groups 3 and 4, most of the best functionals appear to be those with the smallest noninteger subshell occupations. To generalize, it seems that it is necessary to achieve a balanced description of the orbitals before one compares the errors in multiplicity-changing energies, and if a certain functional achieves good accuracy in excitation energy on the basis of significant overstabilization of s or d orbitals, its success should perhaps be considered as resulting from fortuitous cancellation of errors.

Based on this analysis, a final assessment of the overall performance of all the methods is summarized in Table 11. The data used to calculate the errors in Table 11 are composed of

Table 10. MSE and MUE of ΔE for the Variational Method, MUE of ΔE for the WABS Method, and δ of the 5s Subshell Occupation for Group 4

	var		WABS	var		var		WABS	var
functional	MSE	MUE	MUE	δ^a	functional	MSE	MUE	MUE	δ^a
HFLYP	−0.3	0.7	5.9	0.03	LC-ωPBE	−1.0	3.1	6.7	0.22
BMK	−0.7	0.9	6.4	0.08	B3V5LYP	3.2	3.2	2.0	0.11
PW6B95	0.6	1.7	4.6	0.07	B3LYP*	3.2	3.2	2.3	0.12
TPSSh	1.6	1.9	3.2	0.19	B3LYP	3.2	3.2	2.0	0.11
LC-mPWLYP	1.9	1.9	2.9	0.06	MPW3LYP	3.2	3.2	2.0	0.11
revTPSS	1.9	1.9	2.7	0.21	OLYP	3.3	3.3	4.4	0.25
BHandH	−0.9	2.0	6.7	0.06	O3LYP	2.5	3.3	4.4	0.23
BHandHLYP	2.0	2.0	2.7	0.06	B88	−0.9	3.4	6.4	0.34
B98	1.8	2.2	2.9	0.20	GKSVWN3	−1.1	3.5	6.9	0.14
ωB97X	0.9	2.2	3.9	0.21	B1LYP	3.5	3.5	1.6	0.10
TPSS	2.2	2.2	2.3	0.23	SOGGA	−1.2	3.7	7.0	0.20
ωB97X-D	0.5	2.3	4.6	0.12	M06L	3.8	3.8	0.8	0.42
TPSS1KCIS	2.3	2.3	2.5	0.14	M052X	3.2	4.0	5.7	0.26
CAM-B3LYP	2.3	2.3	2.3	0.08	MPWKCIS1K	0.0	4.0	5.3	0.03
M05	0.0	2.6	5.0	0.36	M08-SO	0.9	4.3	5.8	0.22
HSE	−1.0	2.6	6.8	0.08	VS98	−1.5	4.4	7.2	0.27
M06	2.6	2.7	3.4	0.35	OPBE	−1.7	4.5	7.7	0.30
MPWB1K	−1.7	2.7	7.7	0.07	HCHT/407	3.3	4.5	6.4	0.31
SOGGA11-X	−2.6	2.7	8.8	0.12	MOHLYP	4.6	4.6	4.2	0.25
BP86	2.7	2.7	3.3	0.17	MPWLYP1M	4.6	4.6	2.5	0.15
B97-3	2.8	2.8	2.7	0.11	HFPW91	−4.7	4.7	11.7	0.07
SOGGA11	−1.2	2.8	7.1	0.29	BLYP	4.8	4.8	2.5	0.16
B3PW91	−0.1	2.9	5.5	0.13	mPWLYP	4.9	4.9	2.7	0.16
RPBE	1.8	2.9	3.8	0.22	M08-HX	0.2	4.9	6.2	0.32
BPW91	0.9	2.9	4.1	0.21	M11-L	5.7	5.7	3.7	0.38
MPW1K	−1.7	2.9	7.7	0.10	HF	−6.2	6.2	14.2	0.31
N12	0.6	2.9	4.3	0.18	M11	−2.0	6.6	8.7	0.15
τHCTHhyb	1.4	3.0	3.8	0.24	MN12-L	6.9	6.9	4.4	0.21
PBE0	−0.9	3.0	6.6	0.12	M06-2X	9.7	9.7	8.5	0.29
PBE	0.6	3.0	4.6	0.19	M06-HF	18.1	18.1	19.9	0.24
PW91	0.8	3.0	4.3	0.19					

[a] δ denotes the mean unsigned deviation of the four occupancies in group 4 of the 5s subshell from the integer values corresponding to the dominant configuration of the experimental state.

WABS results for group 1 and variational results for groups 2 and 3. The column called "δ" is the mean unsigned deviation from the dominant experimental configuration of 5s occupations in 28 spin states. The columns called "MSE", "MUE(14)", and "MUE(22)" contain respectively the MSE of 14 ΔE's, the MUE of 14 ΔE's, and the MUE of 14 ΔE's plus 8 IPs.

First we consider the MSE results of Table 11. As expected, HF exchange strongly favors HS states with an MSE of −12.0 kcal/mol. Correlation functionals usually favor the LS state, as shown by comparison of the MSE of HF (−12 kcal/mol) with the MSE of HFLYP (1.5 kcal/mol) or HFPW91 (−5.5 kcal/mol) or by comparison of the MSE of B88 (−11.6 kcal/mol) with the MSE of BPW91 (−3.6 kcal/mol) or of BLYP (2.1 kcal/mol). Also, an increased favoring of the HS state is observed when the percentage of Hartree−Fock exchange is increased. This can be most clearly seen in the series of BLYP, B1LYP, and BHandHLYP functionals.

Next we compare MUE(14) and MUE(22) for all the density functionals. This comparison shows that these columns in Table 11 tend to show very similar trends, and therefore we will base our discussion on MUE(22), which is the overall mean unsigned error of all the ΔE's and IPs included in the final analysis based on the considerations above. As expected, the two purely exchange functionals, namely HF and B88, both have large energetic errors, in particular, 18.8 and 11.5 kcal/mol. The best functional is SOGGA11-X with an MUE of 3.1 kcal/mol and a δ of merely 0.01. B1LYP also achieves an MUE of 3.1 kcal/mol but has a slightly larger δ of 0.04. All of the 14 best functionals are hybrid functionals.

Nine of the 10 best performing functionals have a δ equal to or smaller than 0.06, with the only exception being PW6B95. Actually, the δ of 0.18 for PW6B95 is, along with OPBE, the largest of all the 61 tested methods. The best three local functionals, according to excitation energy errors, are revTPSS, RPBE, and TPSS, all of which have large δ values in the range 0.11−0.15. Actually *most* local functionals produce δ equal to or larger than 0.10, with the three exceptions being VS98 (0.05), M11-L (0.08), and BLYP (0.09). Noninteger subshell occupation numbers are problematic; one could consider them to be an undesirable feature, but an alternative interpretation (which at present cannot be ruled out although there is also no evidence to support it) is that noninteger subshell occupancies are a positive feature and represent inclusion of effects that would be labeled as configuration interaction in wave function theory.

If one uses the interpretation that noninteger subshell occupation numbers are to be avoided and considers them in conjunction with the energetic errors, the best local functional appears to be BLYP, which is especially interesting because

Table 11. Overall Performances of All the Methods against Groups 1−3

functional	δ^a	MSE	MUE(14)^b	MUE(22)^c	functional	δ^a	MSE	MUE(14)^b	MUE(22)^c
SOGGA11-X	0.01	2.9	3.4	3.1	PBE	0.11	−2.7	4.4	5.5
B1LYP	0.04	1.5	3.0	3.1	LC-MPWLYP	0.03	5.2	5.4	5.5
B3V5LYP	0.06	1.1	2.9	3.3	BP86	0.11	−1.1	3.7	5.5
MPW3LYP	0.05	1.8	3.1	3.5	PW91	0.12	−2.5	4.3	5.6
B3LYP	0.06	1.2	3.0	3.6	MPW1K	0.09	−5.4	5.5	5.6
CAM-B3LYP	0.03	2.7	3.6	3.6	ωB97X-D	0.02	6.1	6.4	5.9
PW6B95	0.18	1.2	3.2	3.7	BPW91	0.13	−3.6	5.1	6.1
BMK	0.01	3.6	3.6	3.7	M06-L	0.12	4.7	6.2	6.3
BHandH	0.02	−0.1	2.3	3.9	LC-ωPBE	0.09	−1.8	5.7	6.4
B3LYP*	0.06	1.2	3.0	3.9	SOGGA	0.12	−4.3	6.1	6.8
MOHLYP	0.11	2.1	4.1	4.0	SOGGA11	0.12	2.2	7.3	6.8
TPSS1KCIS	0.12	−2.2	4.3	4.1	OPBE	0.18	−2.9	7.4	6.9
TPSSh	0.12	−2.9	4.3	4.2	M08-HX	0.04	5.7	7.7	6.9
MPWKCIS1K	0.05	−2.7	3.9	4.3	τHCTHhyb	0.04	8.0	8.0	7.0
revTPSS	0.14	−2.7	4.4	4.5	MN12-L	0.23	7.5	8.9	7.3
BHandHLYP	0.03	0.9	3.5	4.6	M11	0.05	1.5	6.8	8.1
TPSS	0.15	−2.1	4.3	4.6	HCTH/407	0.1	6.9	7.9	8.1
O3LYP	0.11	1.3	4.9	4.6	M06	0.02	10.0	10.1	8.8
RPBE	0.12	−1.6	3.8	4.6	M06-2X	0.04	11.6	11.6	9.6
PBE0	0.1	−4.5	4.7	4.8	SVWN	0.1	−0.9	5.2	10.4
MPWLYP1M	0.08	2.6	4.0	4.8	HFPW91	0.08	−5.5	6.5	10.4
BLYP	0.09	2.1	4.0	4.9	ωB97X	0.01	11.7	11.7	10.5
HSE	0.08	−4.8	4.8	5.0	HFLYP	0.05	1.5	6.7	10.5
VS98	0.05	1.3	5.4	5.1	M11-L	0.08	7.3	10.5	10.6
B98	0.03	5.7	5.8	5.1	N12	0.2	2.7	10.8	10.6
MPWB1K	0.14	−0.2	2.8	5.2	M05-2X	0.02	11.4	11.9	10.6
B97-3	0.05	5.6	5.8	5.2	M06-HF	0.07	12.1	12.1	11.4
OLYP	0.12	2.5	5.6	5.3	B88	0.14	−11.6	11.6	11.5
M08-SO	0.02	3.0	5.7	5.4	M05	0.01	13.7	13.7	12.1
MPWLYP	0.08	2.8	4.3	5.4	HF	0.14	−12.0	12.1	18.8
B3PW91	0.11	−4.6	5.1	5.4					

$^a\delta$ denotes the mean unsigned deviation of the 28 occupancies of the 5s subshell from the integer values corresponding to the dominant configuration of the experimental state. ^{b}MUE over 14 excitation energies. ^{c}MUE over 14 excitation energies and eight ionization potentials.

some of its hybrid variants, namely, B1LYP, B3V5LYP, B3LYP, CAM-B3LYP, and B3LYP*, are ranked in the top 10 best functionals. However, if one does not penalize noninteger subshell occupancies, the best local functional would be considered to be revTPSS.

Because, as discussed above, Tables 7 and 8 provide very clear-cut tests of the functionals, we might ask which functional has a high rating by all three of the following criteria: columns MUE (WABS) in Table 7, columns MUE (var) in Table 8, and columns MUE(22) in Table 11. We find six functionals are in the top 20 for all of these columns: B3LYP*, B3V5LYP, B3LYP, BHandH, MPWKCIS1K, and SOGGA11-X, and MPW3LYP is always in the top 21. Of these, the highest ranked in the overall MUE(22) columns are SOGGA11-X, B3V5LYP, and MPW3LYP.

Another interesting observation is that the simpler GGA and hybrid GGA functionals tend to perform better than meta-GGA and hybrid meta-GGA functionals. At the meta-GGA or hybrid meta-GGA level, there is only one functional with a low MUE in excitation energies and a low δ, namely BMK. Other than BMK, other meta-GGAs and hybrid meta-GGAs with relatively small MUEs, such as PW6B95 and several variants of TPSS, are all observed to have very large δ; ones with small δ, including M05, M06, and M06-2X, all perform unsatisfactorily for excitation energies.

Finally, we compare the conclusions reached here to those in a closely related study, namely a study[9] of p-block excitation energies that allowed an assessment the accuracy of self-consistent calculations on states of different multiplicities without the complications of broken symmetry, multireference character or d orbitals. Therefore the tests were interpreted as a rather clean test of high-spin bias vs low-spin bias. Of the functionals included here, the ones that performed best overall in ref 9 are O3LYP, TPSS, M06-2X, and CAM-B3LYP. Table 9 shows that three of these are also above average for 4d transition metals, but M06-2X becomes poor, which is consistent with our previous experience that caused us to recommend that M06-2X not be used for transition metals.

6. CONCLUSIONS

We summarize this paper with the following remarks:

(i) For subshell occupation numbers, section 5.1 shows that local functionals tend to overstabilize 4d orbitals over 5s orbitals, and HF exchange tends to alleviate this bias. For excitation energy differences, Table 10 shows that correlation functionals in DFT usually favor the LS state, while HF exchange favors the HS state. Therefore, to achieve a well-balanced description of both occupations and excitation energies in 4d transition metals, an appropriate percentage of HF exchange is necessary.

(ii) GGAs and their hybrid variants perform better than functionals built at the meta-GGA and hybrid meta-GGA levels, which seems to leave room for further improvements of present meta-GGAs and hybrid meta-GGAs.

(iii) The ranking of functions in the final overall assessment is not well correlated with the percentage of HF exchange.

(iv) SOGGA11-X and B1LYP offer good accuracy in both subshell occupations and excitation energies and have the lowest mean unsigned error in the final overall evaluation, B3V5LYP and MPW3LYP perform almost as well as B1LYP, and B3LYP, CAM-B3LYP, BMK, and PW6B95 rank in the next four positions. Thus these eight functionals are recommended for accurate calculations of spin states and ionization potentials of 4d elements.

APPENDIX

The derivation of eq 3 begins with the assumption that the orbitals in the HS and LS states are similar so that the BS state is a linear combination of determinants with the same orbitals (but different spin-coupling) as the HS state. In such a case we can use the phenomenological Heisenberg Hamiltonian:

$$\hat{H} = J\hat{S}^2 \tag{A1}$$

in which J is a phenomenological constant and $\hat{S}^2$ is the total electron spin, and for which the expectation value of the energy is

$$E = J\langle\hat{S}^2\rangle \tag{A2}$$

and the energy eigenvalues are

$$E = JS(S+1) \tag{A3}$$

where S is the total spin quantum number. In the present article we always have S_{LS} equal to $S_{HS} - 1$. Therefore

$$E_{HS} = JS_{HS}(S_{HS}+1) \tag{A4}$$

$$E_{LS} = JS_{HS}(S_{HS}-1) \tag{A5}$$

and

$$\Delta E = E_{HS} - E_{LS} = 2JE_{HS} \tag{A6}$$

But eq A2 yields

$$J = \frac{E_{HS} - E_{LS}}{\langle\hat{S}^2\rangle_{HS} - \langle\hat{S}^2\rangle_{LS}} \tag{A7}$$

Combining eqs A6 and A7 and relabeling the LS state as BS yields eq 3.

AUTHOR INFORMATION

Notes

The authors declare no competing financial interest.

ACKNOWLEDGMENTS

The authors are grateful to Boris Avenkiev and Ke Yang for helpful discussions. This work was supported in part by the AFOSR and the NSF.

REFERENCES

(1) Kohn, W.; Sham, L. *Phys. Rev.* **1964**, *140*, A1133.
(2) Barth, U.; Hedin, L. A. *J. Phys. C* **1972**, *5*, 1629.
(3) Seidl, A.; Görling, A.; Vogl, P.; Majewski, J. A.; Levy, M. *Phys. Rev. B* **1996**, *53*, 3764.
(4) Cramer, C. J.; Truhlar, D. G. *Phys. Chem. Chem. Phys.* **2009**, *11*, 10757.
(5) Moore, C. E. *Atomic Energy Levels*; National Bureau of Standards: Washington, DC, 1949−1958, Vols. *1*−*3*.
(6) (a) Noodleman, L. *J. Chem. Phys.* **1981**, *74*, 5737. (b) Bachler, V.; Olbrich, G.; Neese, F.; Wieghardt, K. *Inorg. Chem.* **2002**, *41*, 4179.
(7) Neese, F. *Coord. Chem. Rev.* **2009**, *253*, 526.
(8) (a) Yamaguchi, K.; Takahara, Y.; Fueno, T. In *Applied Quantum Chemistry*; Smith, V. H., Jr., Schaefer, H. F., III, Morokuma, K., Eds.; D. Reidel: Boston, 1986; p 155. (b) Caballol, R.; Castell, O.; Illas, F.; de P. R. Moreira, I.; Malrieu, J. P. *J. Phys. Chem.* **1997**, *101*, 7860. (c) Shoji, M.; Koizumi, K.; Kitagawa, Y.; Kawakami, T.; Yamanaka, S.; Okumura, M.; Yamaguchi, K. *Chem. Phys. Lett.* **2006**, *432*, 343.
(9) Yang, K.; Peverati, R.; Truhlar, D. G.; Valero, R. *J. Chem. Phys.* **2011**, *135*, 044118.
(10) Yanagisawa, S.; Tsuneda, T.; Hirao, K. *J. Chem. Phys.* **2000**, *112*, 545.
(11) Gáspár, R. *Acta Phys. Hung.* **1974**, *35*, 213.
(12) Vosko, S. H.; Wilk, L.; Nusair, M. *Can. J. Phys.* **1980**, *58*, 1200.
(13) Becke, A. D. *Phys. Rev. A* **1988**, *38*, 3098.
(14) Lee, C.; Yang, W.; Parr, R. G. *Phys. Rev. B* **1988**, *37*, 785.
(15) Perdew, J. P. *Phys. Rev. B* **1986**, *33*, 8822.
(16) Perdew, J. P. In *Electronic Structure of Solids '91*; Ziesche, P., Eschrig, H., Eds.; Akademie Verlag: Berlin, 1991; pp 11−20.
(17) Hamprecht, F. A.; Cohen, A.; Tozer, D. J.; Handy, N. C. *J. Chem. Phys.* **1998**, *109*, 6264.
(18) Boese, A. D.; Handy, N. C. *J. Chem. Phys.* **2001**, *114*, 5497.
(19) Adamo, C.; Barone, V. *J. Chem. Phys.* **1998**, *108*, 664.
(20) Handy, N. C.; Cohen, A. J. *Mol. Phys.* **2001**, *99*, 403.
(21) Perdew, J. P.; Burke, K.; Ernzerhof, M. *Phys. Rev. Lett.* **1996**, *77*, 3865.
(22) Hammer, B.; Hansen, L. B.; Norskov, J. K. *Phys. Rev. B* **1999**, *59*, 7413.
(23) Zhao, Y.; Truhlar, D. G. *J. Chem. Phys.* **2008**, *128*, 184109.
(24) Peverati, R.; Zhao, Y.; Truhlar, D. G. *J. Phys. Chem. Lett.* **2011**, *2*, 1911.
(25) Peverati, R.; Truhlar, D. G. *J. Chem. Theory Comput.* **2012**, *8*, 2310.
(26) Adamo, C.; Barone, V. *Chem. Phys. Lett.* **1997**, *274*, 242.
(27) Stephens, P. J.; Devlin, F. J.; Chabalowski, C. F.; Frisch, M. J. *J. Phys. Chem.* **1994**, *98*, 11623.
(28) Reiher, M.; Salomon, O.; Hess, B. A. *Theor. Chem. Acc.* **2001**, *107*, 48.
(29) Becke, A. D. *J. Chem. Phys.* **1993**, *98*, 5648.
(30) Hertwig, R. H.; Koch, W. *Chem. Phys. Lett.* **1997**, *268*, 345.
(31) Keal, T. W.; Tozer, D. J. *J. Chem. Phys.* **2005**, *123*, 121103.
(32) Schmider, H. L.; Becke, A. D. *J. Chem. Phys.* **1998**, *108*, 9624.
(33) Becke, A. D. *J. Chem. Phys.* **1993**, *98*, 1372.
(34) Schultz, N. E.; Zhao, Y.; Truhlar, D. G. *J. Phys. Chem. A* **2005**, *109*, 11127.
(35) Lynch, B. J.; Fast, P. L.; Harris, M.; Truhlar, D. G. *J. Phys. Chem. A* **2000**, *104*, 4811.
(36) Zhao, Y.; Truhlar, D. G. *J. Phys. Chem. A* **2004**, *108*, 6908.
(37) Zhao, Y.; Lynch, B. J.; Truhlar, D. G. *J. Phys. Chem. A* **2004**, *108*, 4786.
(38) Hoe, M. W.; Cohen, A. J.; Handy, N. C. *Chem. Phys. Lett.* **2001**, *341*, 319.
(39) Adamo, C.; Barone, V. *J. Chem. Phys.* **1999**, *110*, 6158.
(40) Peverati, R.; Truhlar, D. G. *J. Chem. Phys.* **2011**, *135*, 191102.
(41) Yanai, T.; Tew, D. P.; Handy, N. C. *Chem. Phys. Lett.* **2004**, *393*, 51.
(42) Heyd, J.; Scuseria, G. E.; Ernzerhof, M. *J. Chem. Phys.* **2003**, *118*, 8207.
(43) Henderson, T. M.; Izmaylov, A. F.; Scalmani, S.; Scuseria, G. E. *J. Chem. Phys.* **2009**, *131*, 044108.
(44) Iikura, H.; Tsuneda, T.; Yanai, T.; Hirao, K. *J. Chem. Phys.* **2001**, *115*, 3540.
(45) Vydrov, O. V.; Scuseria, G. E. *J. Chem. Phys.* **2006**, *125*, 234109.
(46) Chai, J.; Head-Gordon, M. *J. Chem. Phys.* **2008**, *128*, 084106.
(47) Chai, J.; Head-Gordon, M. *Phys. Chem. Chem. Phys.* **2008**, *10*, 6615.
(48) Zhao, Y.; Truhlar, D. G. *J. Chem. Phys.* **2006**, *125*, 194101.
(49) Peverati, R.; Truhlar, D. G. *J. Phys. Chem. Lett.* **2012**, *3*, 117.

(50) Perdew, J. P.; Ruzsinszky, A.; Csonka, G. I.; Constantin, L. A.; Sun, J. *Phys. Rev. Lett.* **2009**, *103*, 026403.
(51) Tao, J.; Perdew, J. P.; Staroverov, V. N.; Scuseria, G. E. *Phys. Rev. Lett.* **2003**, *91*, 146401.
(52) Van Voorhis, T.; Scuseria, G. E. *J. Chem. Phys.* **1998**, *109*, 400.
(53) Peverati, R.; Truhlar, D. G. *Phys. Chem. Chem. Phys.* **2012**, *14*, 13171.
(54) Boese, A. D.; Martin, J. M. L. *J. Chem. Phys.* **2004**, *121*, 3405.
(55) Zhao, Y.; Schultz, N. E.; Truhlar, D. G. *J. Chem. Phys.* **2005**, *123*, 161103.
(56) Zhao, Y.; Schultz, N. E.; Truhlar, D. G. *J. Chem. Theory Comput.* **2006**, *2*, 364.
(57) Zhao, Y.; Truhlar, D. G. *Theor. Chem. Acc.* **2008**, *120*, 215.
(58) Zhao, Y.; Truhlar, D. G. *J. Phys. Chem. A* **2006**, *110*, 13126.
(59) Zhao, Y.; Truhlar, D. G. *J. Chem. Theory Comput.* **2008**, *4*, 1849.
(60) Krieger, J. B.; Chen, J.; Iafrate, G. J.; Savin, A. In *Electron Correlations and Materials Properties*; Gonis, A., Kioussis, N., Eds.; Plenum: New York, 1999; p 463.
(61) Zhao, Y.; González-García, N.; Truhlar, D. G. *J. Phys. Chem. A* **2005**, *109*, 2012.
(62) Zhao, Y.; Truhlar, D. G. *J. Phys. Chem. A* **2005**, *109*, 5656.
(63) Zhao, Y.; Lynch, B. J.; Truhlar, D. G. *Phys. Chem. Chem. Phys.* **2005**, *7*, 43.
(64) Staroverov, V. N.; Scuseria, G. E.; Tao, J.; Perdew, J. P. *J. Chem. Phys.* **2003**, *119*, 12129.
(65) Boese, A. D.; Handy, N. C. *J. Chem. Phys.* **2002**, *116*, 9559.
(66) Peverati, R.; Truhlar, D. G. *J. Phys. Chem. Lett.* **2011**, *2*, 2810.
(67) Frisch, M. J.; Trucks, G. W.; Schlegel, H. B.; et al. *Gaussian 09*, revision C.1; Gaussian, Inc., Wallingford, CT, 2009.
(68) Foster, J. P.; Weinhold, F. *J. Am. Chem. Soc.* **1980**, *102*, 7211.
(69) Reed, A. E.; Weinhold, F. *J. Chem. Phys.* **1983**, *78*, 4066.
(70) Reed, A. E.; Weinstock, R. B.; Weinhold, F. *J. Chem. Phys.* **1985**, *83*, 735.
(71) Reed, A. E.; Weinhold, F. *J. Chem. Phys.* **1985**, *83*, 1736.
(72) Carpenter, J. E. Ph.D. Thesis, University of Wisconsin, Madison, WI, 1987.
(73) Carpenter, J. E.; Weinhold, F. *J. Mol. Struct.: THEOCHEM* **1988**, *46*, 41.
(74) Reed, A. E.; Curtiss, L. A.; Weinhold, F. *Chem. Rev.* **1988**, *88*, 899.
(75) Weinhold, F.; Carpenter, J. E. In *The Structure of Small Molecules and Ions*; Naaman, R., Vager, Z., Eds.; Plenum: New York, 1988; pp 227−236.
(76) Douglas, M.; Kroll, N. M. *Ann. Phys.* **1974**, *82*, 89.
(77) Hess, B. A. *Phys. Rev. A* **1986**, *33*, 3742.
(78) Jansen, G.; Hess, B. A. *Phys. Rev. A* **1989**, *39*, 6016.
(79) Peterson, K. A.; Figgen, D.; Dolg, M.; Stoll, H. *J. Chem. Phys.* **2007**, *126*, 124101.
(80) Tsuchiya, T.; Abe, M.; Nakajima, T.; Hirao, K. *J. Chem. Phys.* **2001**, *115*, 4463.
(81) Huzinaga, S.; Klobukowski, M. *Chem. Phys. Lett.* **1993**, *212*, 260.
(82) Roos, O.; Lindh, R.; Malmqvist, P. A.; Veryazov, V.; Widmark, P. O. *J. Phys. Chem. A* **2005**, *109*, 6575.
(83) Gunnarsson, O.; Jones, R. O. *Phys. Rev. B* **1985**, *31*, 7588.